한국지반환경공학회 논문집 제7권 제2호 2006년 4월 pp. 43~53

Study on the Fracture Deformation Characteristics in Rock by Hydraulic Fracturing

수압파쇄에 의한 암반 균열의 변형 특성 연구

Sim, Young-Jong* · Kim, Hong-Taek** · Leonid N. Germanovich***
심영종 · 김홍택 · Leonid N. Germanovich

Abstract

Hydraulic fracturing is an important and abundant process in both industrial applications and natural environments. The formation of hydraulic fractures includes nucleation, growth, and termination in numerous rock types and stress regimes, at scales ranging from microns to many kilometers. As a result, fracture segmentation, commonly observed at all scales and in all geo-materials, contributes to this complexity in many ways. In particular, the mechanical interaction of fracture segments strongly affect almost all hydraulic fracturing processes. In this paper, the segmented fracture opening deformation in rock by hydraulic fracturing is quantified using boundary collocation method and is compared with non-interacting single fracture.

Keywords: Hydraulic Fracturing, Mechanical Interaction, Segmentation, Fracture Opening Deformation

요 지

수압파쇄(hydraulic fracturing)는 자연환경에서 흔히 일어나는 현상이며 산업현장에서도 많이 응용되는 방법 중의 하나이다. 수압파쇄는 다양한 암반과 응력 상태에서 균열이 생성되어 전파하며 지극히 작은 축척에서부터 수 킬로미터에 이르는 대규모 축척까지 다양한 형태로 나타난다. 그 결과 균열은 복잡한 형태의 기하를 나타내며 그 거동 또한 복잡한 양상을 띠게 된다. 특히 다중으로 분할된 형태의 균열은 흔히 모든 축척과 지반재료에서 나타나며 이러한 복잡한 거동의 한 부분을 차지한다. 특히 이러한 균열 간의 기계적 상호작용은 거의 모든 수압파쇄 과정에 영향을 끼친다. 따라서 이 논문에서는 수압파쇄에 의해 암반에서 생성되는 균열의 변형을 경계병치법을 사용하여 정량화하였으며 기계적 상호작용을 고려치 않은 단균열의 경우와 비교하였다.

주요어 : 수압파쇄, 기계적 상호작용, 분할, 균열폭 변형

* Member, Post-Doctoral Fellow, Civil and Environmental Engineering, KAIST, yjsim@kaist.ac.kr

** Member, Professor, Civil Engineering, Hong-Ik University

*** Professor, Civil and Environmental Engineering, Georgia Tech.

1. INTRODUCTION

During the last few decades, hydraulic fracturing has been a widely used technology for oil and gas recovery (e.g., Economides and Nolte, 2000), geothermal heat extraction (e.g., Nemat-Nasser,1983), in-situ stress measurement (e.g., Shin et al., 2001), waste disposal (e.g., Keck et al., 1996), coal degasification in advance of mining (e.g., Palmer and Sparks, 1991), and remediation of contaminated water (e.g., Murdoch and Slack, 2002). Obtaining proper results by hydraulic fracturing (in the petroleum engineering in particular) depends highly on the geometric configuration of the fracture and the stress regime in the subsurface. This is why hydraulic fracturing has been a subject of active research to clarify the mechanisms of fluid-rock (or sediment) interaction. The geometry of the hydraulic fractures is affected by mechanical, thermal, and chemical conditions of the surrounding host rock. This can result in complicated structures deep in the subsurface or near the surface. Therefore, understanding the fracturing processes by fluid injection is of practically great importance for maximizing its effectiveness.

In nature, hydraulic fractures also appear in a variety of forms, such as sheet intrusions (i.e., sills and dikes), veins, and even joints. In many aspects, the mechanical behavior of natural hydraulic fractures is analogous to that of fracture propagation in industrial hydraulic fracturing since natural hydraulic fractures are created in the host rock by opening mode (referred to as dilatant, tensile, or extensional mode by different authors) driven by the internal pressure of fluids (e.g., magma, water, gas, or an aqueous solution), remote stress (e.g., tectonic stress), or a combination of both.

These natural opening mode fractures are frequently found in the earth's crust. The formation of these fractures includes nucleation, dilation, propagation and termination in a variety of rock types and stress regimes at scales ranging from microns to many kilometers. As a result, the fractures show complicated geometrical features such as multiple segments.

Segmentation is indeed one of the most often encountered features contributing to the complexity of hydraulic fractures. Recent observations based on geological evidence, laboratory experiments, and mineback observations confirm that the occurrence of multisegmented hydraulic fractures (MHF) is a common phenomenon. However, current hydraulic fracture models presume a single fracture or neglect mechanical interaction between multiple fractures that dramatically changes hydraulic fracturing parameters such as fracture aperture, length, and net pressure (Astakhov, 2000). In an attempt to gain insight into the causes of MHF, the next section focuses on observations of MHF in nature, laboratory experiments, and industrial observations.

2. OBSERVATIONS OF THE MHF

2.1 MHF in nature

As stated earlier, hydraulic fractures in nature appear in a variety of forms, such as sheet intrusions, veins, and even joints. Sheet intrusions, such as vertical dikes and horizontal sills, are related to the magma fluid. If the magma fluid pressure is sufficiently high to overcome the in-situ compressive stress and rock strength, it splits the host rock (e.g., Anderson, 1938; Hubbert and Willis, 1957). On the basis of observations of the geometric features of sheet intrusions, segmentations with consecutive overlapping are common phenomena for many types of rock. Figure 1a shows a part of northeastern minette dike segments found near Ship Rock in New Mexico (Delaney and Pollard, 1981). The dike has an outcrop length of 2,900 m and maximum aperture of 7.2 m, and

is composed of 35 distinct segments. It is generally known that the single parent dike begins to break into several segments when it encounters a region in which the direction of least principal stress is rotated about the axis of propagation direction as illustrated in Figure 1b (Delaney and Pollard, 1981). For this reason, the segments show oblique-segmented geometric features relative to the parent dike, which is called en echelon.

Veins are composed of one or more minerals that precipitated from the hydrothermal solution that flows through a rock by diffusion, advection, or hydraulic fracturing (Fisher and Brantley, 1992). Although the formation of veins is not clearly understood, it is likely to be highly dependent upon the subsurface structures such as voids, fractures, and faults. Various types of veins are found in nature. En echelon veins are found in rocks as well. Figure 1c shows en echelon vein arrays.

Joints, the most common brittle structure in the Earth's crust (Pollard and Aydin, 1988), can be formed by remote extension or hydraulic fracturing (Secor, 1965). Multiple joints are also commonly found in nature. Figure 1d shows a well-exposed set of parallel joints in the dolomite layers of Argot stream, central Dead Sea basin. The significant mechanical interaction during formation can be expected because the spacing of the joints is relatively small compared to their length.

(a) Minette dike segments at a scale of several kilometer near Ship Rock, New Mexico (Delaney and Pollard, 1981)

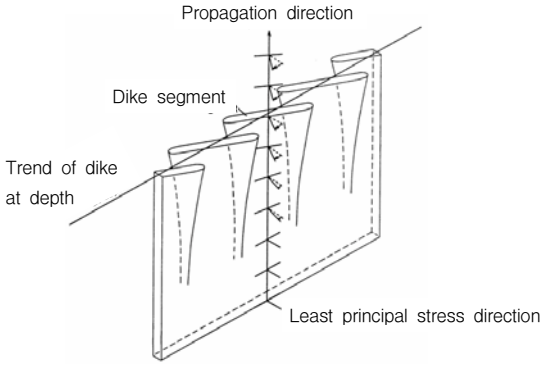

(b) Formation of segmented dike due to rotation of the least compressive stress direction (Delaney and Pollard, 1981)

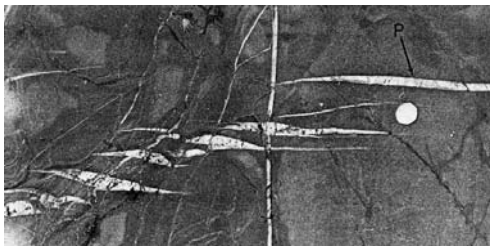

(c) En echelon veins in Millook Haven, S.W. England (Beach, 1977)

(d) Parallel joints set in the dolomite layer of Argot stream, central Dead Sea basin (Sagy et al., 2001)

Figure 1. MHF in nature

2.2 MHF in laboratory experiment and industrial field

Numerous papers have been devoted to laboratory experiments of hydraulic fracturing, investigating the dimensions of hydraulic fractures, and identifying the mechanisms of fracture growth. The results of many experiments have clearly shown the existence of MHF. For example, Dudley et al. (1995) conducted an extensive laboratory investigation of hydraulic fracturing to identify various fracture mechanisms that may also affect and control the growth of large-scale hydraulic fractures in the field. The observed patterns of hydraulic fracture growth in sandstone specimens, which is relatively homogeneous rock, are fracture branching (Figure 2a), bridging of the fracture faces, and formation of micro fractures in the vicinity of the main fracture surface.

It is expected that multiple segments are more likely to form in experiments in heterogeneous materials than in homogeneous media. The interfaces and discontinuities, such as joints, fissures, faults, and bedding planes, that are the most common features in natural rocks, affect hydraulic fracture growth in conjunction with tectonic stress. For example, Figure 2b shows the result of an experiment conducted by Hanson et al. (1981) to identify the effect of low friction on the hydraulic fracture growth across an unbonded interface. The three-block limestone has been stacked in a press. An internal pressure was applied to force the fractures to propagate across the interfaces. The upper interface has lower frictional properties than the lower one. As a result, hydraulic fracture propagated across the upper interface with a lateral offset, while it propagated directly through the lower interface. This result shows that frictional properties at the interface affect the geometry of fracture growth.

Direct observations from mineback experiments in the field also reveal that hydraulic fractures rarely, if ever, propagate as a single planar feature. Hydraulic fracturing is commonly conducted at the field scale for degasification from coal beds in advance of mining. Hence, it is possible to make a detailed mapping of exposed hydraulic fractures in a coal seam by mining operations. Palmer and Sparks (1991) observed the height and width of hydraulic fractures in Black Warrior basin coalbeds in Alabama. They used downhole visual logging to better understand fracturing behavior. Figure 2c shows one of the propped fractures in the coal seam and surrounding rock strata through downhole visual logging.

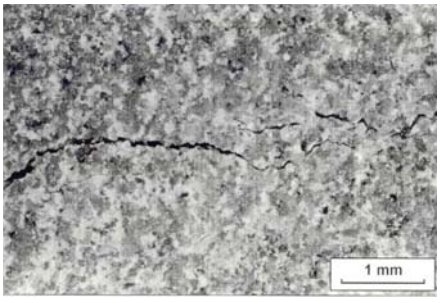

(a) Hydraulic fracture branching in sandstone (Dudley et al., 1995)

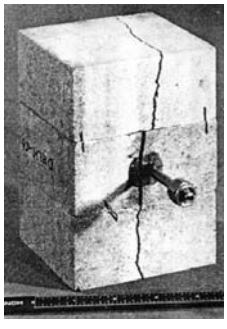

(b) Lateral offset of hydraulic fracture across an unbonded interface of limestone (Hanson et al., 1981)

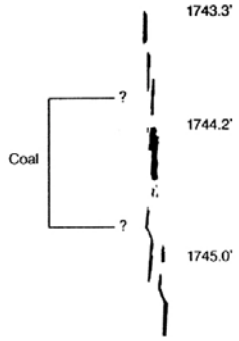

(c) Multiple fractures in a coal seam and surrounding strata (Palmer and Sparks, 1991)

Figure 2. MHF in lab experiment and field

3. ELASTIC INTERACTION BETWEEN MULTIPLE FRACTURES

The problem of multiple defects has been a key issue in many disciplines, because elastic interaction significantly changes the stress and strain fields in materials. In the field of hydraulic fracturing, the opening across a fracture are of great concern in the evaluation of hydraulic fracturing parameters (e.g., Naceur and Roegiers, 1990; Germanovich et al., 1998) that are significantly affected by the mechanical interaction between the segments. Because analytical solutions are seldom feasible, many authors have addressed this problem numerically (e.g., Erdogan and Gupta, 1972; McCartney and Gorley, 1987).

This section describes a numerical formulation for analyzing the elastostatic fracture-induced stress fields for arbitrarily arranged, multiple, non-intersecting fractures in a homogeneous plane. A boundary collocation method (BCM), which has been used for the solution of problems with multiple cracks (e.g., McCartney and Gorley, 1987) is employed to accurately evaluate the opening displacements. In this method, the prescribed boundary conditions are satisfied in a finite number of collocation points using Chebyshev polynomials as approximating functions (e.g., Gladwell and England, 1977; McCartney and Gorley, 1987).

First, consider a pair of fractures ($N=2$) in an infinite plane that are located at $z_1 = x_1 + iy_1$ and $z_2 = x_2 + iy_2$, respectively (Figure 3). Known tractions $p_1(z_1) = \sigma_1 + i\tau_1$ and $p_2(z_2) = \sigma_2 + i\tau_2$ are applied to the first and second fracture where σ and τ are the normal and shear traction components, respectively. Based on the superposition principle, this problem can be represented as a sum of two auxiliary problems for a single fracture (Figure 3). In the first auxiliary problem, unknown tractions acting on the first fracture $q_1 = s_1 + it_1$ induce stresses $\Delta q_1 = \Delta s_1 + i\Delta t_1$ at the location of the second fracture. Likewise, in the second auxiliary problem, unknown tractions loading the second fracture $q_2 = s_2 + it_2$ generate stresses $\Delta q_2 = \Delta s_2 + i\Delta t_2$ at the location of the first fracture. Therefore, the tractions in the original problem can be written as:

$$q_1(z_1) + \Delta q_2(z_1) = p_1(z_1),$$
$$q_2(z_2) + \Delta q_1(z_2) = p_2(z_2) \quad (1)$$

Representing the unknown tractions q_1 and q_2 in (1) in the form of the Chebyshev polynomial expansions gives

$$q = s + it = -\sum_{m=1}^{M} (\alpha_m + i\beta_m) U_{m-1}(\xi),$$
$$(-1 < \xi < 1) \quad (2)$$

where α_m and β_m are real unknown coefficients that need to be determined, M is the number of collocation points (which may be different for each fracture), $U_m(\xi) = \sin((m+1)\arccos(\xi))/\sin(\arccos(\xi))$ is the mth order Chebyshev polynomial of the second kind, $\xi = x/c$ is the dimensionless spatial coordinate along the fracture, and c is the alf-size of the fracture. For the auxiliary problems, the second terms, Δq_1 and Δq_2, in (1)

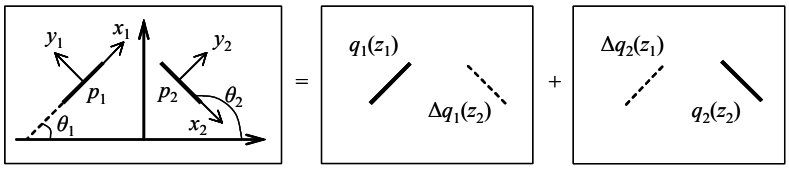

Figure 3. Original and auxiliary problems for interacting fractures.

hthat represent the effect of interaction can be calculated as follows (Muskhelishvili, 1953):

$$\triangle q = \Phi(z) + \overline{\Phi(z)} + e^{2i\theta}[\overline{\Phi(\overline{z})} - \Phi(z) - (z-\overline{z})\Phi'(z)] \quad (3)$$

where θ is the inclination angle of the fracture with respect to the global coordinate set (Figure 1). The complex potential $\Phi(z)$ is expressed as (Muskhelishvili, 1953):

$$\Phi(z) = \frac{1}{2\pi\sqrt{z^2-c^2}} \int_{-c}^{c} \frac{\sqrt{c^2-t^2}}{t-z} \overline{q(t)} dt \quad (4)$$

Using the Gauss-Chebyshev integration formula (e.g., Gladwell and England, 1977)

$$-\frac{1}{\pi}\int_{-1}^{1} \frac{\sqrt{1-\xi^2}}{\xi-\zeta} U_{m-1}(\xi) d\xi = [\zeta - \sqrt{\zeta^2-1}]^m,$$
$$|\xi| \le 1, \ m \ne 0 \quad (5)$$

for singular integrals and taking into account (2), the Muskhelishvili (1953) potential (4) can be expressed in the following form

$$\Phi(\zeta) = \frac{1}{2\sqrt{\zeta^2-1}} \sum_{m=1}^{M} (\alpha_m - i\beta_m)[\zeta - \sqrt{\zeta^2-1}]^m \quad (6)$$

where $\zeta = z/c = \xi + i\eta$, $\xi = x/c$, and $\eta = y/c$. Therefore, based on (3), the auxiliary stress Δq can be also expressed in terms of the coefficients α_m and β_m. Finally, (1) forms a linear system of equations with the number of equations depending on the total number of collocation points. Solving this system produces the unknown coefficients α_m and β_m. Similarly, for the N-fracture problem, the general relationship between all tractions can be written as a sum of N auxiliary problems.

After the unknown real coefficients α_m and β_m are determined by solving linear system of equations, the fracture opening and stress intensity factors can be calculated easily. Therefore, the fracture opening is given by

$$\triangle v + i\triangle u = \frac{4c}{E_1}\sqrt{1-\xi^2} \sum_{m=1}^{M} \frac{1}{m}(\alpha_m + i\beta_m) U_{m-1}(\xi) \quad (7)$$

and the stress intensity factors are expressed as

$$K_I + iK_{II} = \sqrt{\pi c} \sum_{m=1}^{M} (\pm 1)^{m+1}(\alpha_m + i\beta_m) \quad (8)$$

where $G = E/[2(1+\nu)]$ is the shear modulus, ν =Poisson's ratio, κ=3 - 4ν, and $E_1 = E/(1-\nu^2)$ (since only the plane strain case is considered), and "+" and " - " in (8) indicate the stress intensity factors for the crack tips with $\xi > 0$ and $\xi < 0$, respectively.

4. FRACTURE OPENING DEFORMATION IN ROCK

4.1 Single non-interacting hydraulic fracture

For the sake of evaluating the effect of segment interaction, the single non-interacting fractures need to be considered. In this case, each segment is treated as a mechanically isolated fracture. The normal fracture opening, $\Delta v_s = v_s^+ - v_s^-$ of a single isolated fracture with a length of 2c, under the influence of a net pressure Δp (i.e., the difference between the internal pressure p and the remote stress σ_∞), in an infinite, homogeneous, and isotropic medium, is given by (e.g., Tada et al., 1985)

$$\triangle v_s = 4c\frac{\triangle p}{E_1}\sqrt{1-\frac{x^2}{c^2}}, \ |x| \le c \quad (9)$$

If a single net pressure Δp is used, the opening of the segment is simply elliptical.

4.2 Fully opened and partially closed MHF

In this section, examples of the MHF geometries are given for the purpose of understanding the effect of interaction between segments. The geometry and opening of six segments (Table 1) for zero shear tractions and equal pressures (normal traction) inside the segments, $p_1 = p_2 = p_3 = p_4 = p_5 = p_6 = 1.0$ Pa, no remote stresses, $\sigma_{xx}^{\infty} = \sigma_{yy}^{\infty} = \tau_{xy}^{\infty} = 0$ are shown in Figure 4. Elastic properties, Poisson's ratio, $\nu = 0.21$, and Young's modulus, $E = 2.5 \times 10^{10}$ Pa, are selected to calculate fracture opening. The number of collocation points on the segments are $M_1 = 23$, $M_2 = 20$, $M_3 = 35$, $M_4 = 28$, $M_5 = 31$, and $M_6 = 25$, respectively. All six segments are open.

Table 1. Configuration of six segments.

Segment	Center of segment (x(m), y(m))	Inclination angle (deg)	Half length (m)
1	(1.85, 0.4)	0	1.125
2	(0.3, 0.9)	80	0.750
3	(1.5, 1.9)	90	1.0
4	(1.8, 1.9)	90	1.0
5	(2.1, 1.9)	90	1.0
6	(2.4, 1.9)	90	0.875

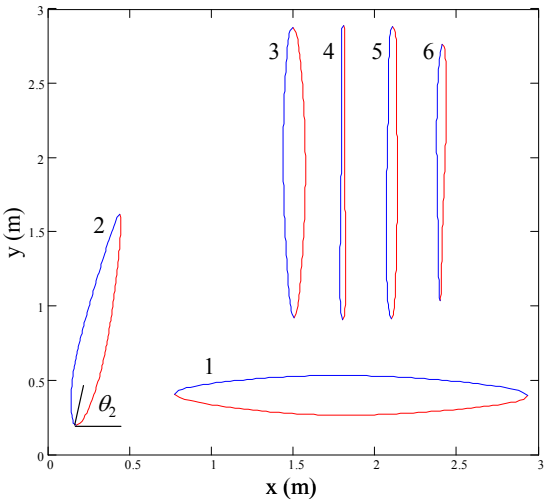

Figure 4. Fully opened MHF geometry and opening

For the comparison of the opening deformation with non-interacting single segment, normalized openings of interacting segments are shown in Figure 5a. Normalizing the segment openings by the opening of the same segment in non-interacting setting (9) allows clearly see the effect of segment interaction. Since both interacting and non-interacting segments are loaded by the same pressure, the segments with openings smaller than 1 are contracted by the interaction while the segments with opening greater than 1 are dilated as a result of the interaction. Not normalized openings of the same fracture configuration are also shown in Figure 5b. This figure allows seeing the actual segment openings in which segment is wider.

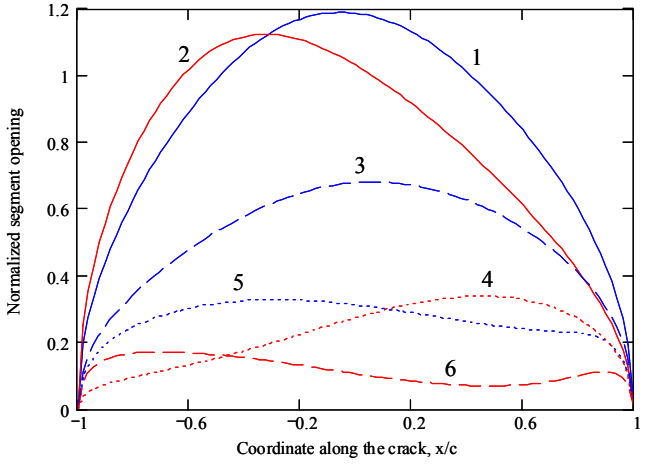

(a) Normalized segment opening

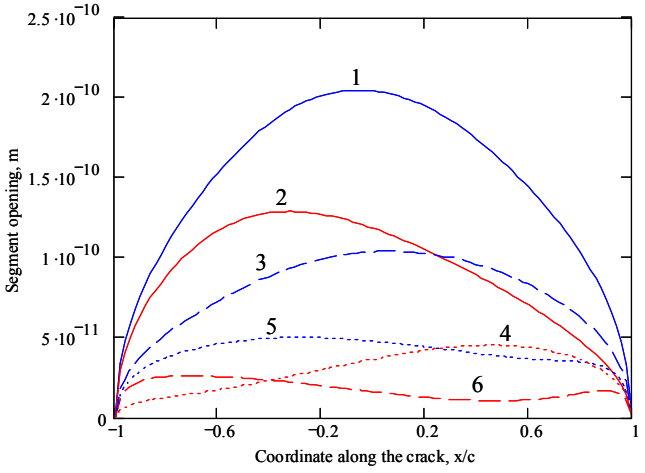

(b) Actual segment opening

Figure 5. Segment opening for fully opened MHF

The different actual opening in the same segments with pressures (normal tractions) inside the segments, $p_1 = 2.0$ Pa, $p_2 = 1.0$ Pa, $p_3 = 1.3$ Pa, $p_4 = p_5 = 1.25$ Pa, $p_6 = 1.3$ Pa, shear tractions on the segment sides, $\tau_1 = \tau_5 = -0.25$ Pa, $\tau_2 = -1.0$ Pa, $\tau_3 = 0.25$ Pa, $\tau_4 = 0.5$ Pa, $\tau_6 = -0.5$ Pa, remote stresses, $\sigma_{xx}^{\infty} = -0.25$ Pa, $\sigma_{yy}^{\infty} = -0.75$ Pa, $\tau_{xy}^{\infty} = 0.5$ Pa are shown in Figure 6. In this condition, segments 4 and 5 have interpenetrated sides that are interpreted as partial closure of real segments. It can be concluded that the MHF may be fully opened or partially closed with different pressure application in the same setting due to the change of degree of interaction.

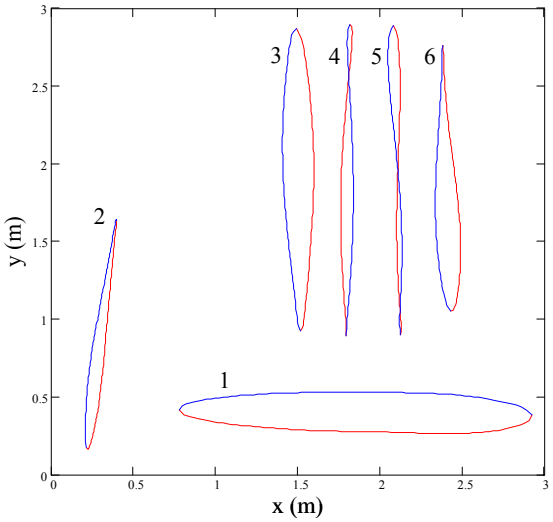

Figure 6. Partially closed MHF geometry and opening

4.3 Consecutive overlapping MHF

All five overlapping segments (Table 2) have different sizes and are loaded by the same pressure, $p_1 = p_2 = p_3 = p_4 = p_5 = 1.0$ Pa (zero shear tractions on segment sides) as in Figure 7. In fact, this type of segmentation with consecutive overlapping represents important frequent elements in the field (see Figure 1a and Figure 1c). Poisson's ratio and Young's modulus are $\nu = 0.21$ and $E = 2.5 \times 10^{10}$ Pa, respectively. The number of collocation points on the segments are $M_1 = 32$, $M_2 = 30$, $M_3 = 37$, $M_4 = 35$, and $M_5 = 40$, respectively.

Table 2. Configuration of five parallel overlapping segments.

Segment	Center of segment (x(m), y(m))	Inclination angle (deg)	Half length (m)
1	(3.00, 2.50)	55	2.50
2	(5.00, 6.00)	55	2.25
3	(7.30, 10.00)	55	3.25
4	(9.80, 14.50)	55	3.00
5	(12.70, 19.40)	55	3.50

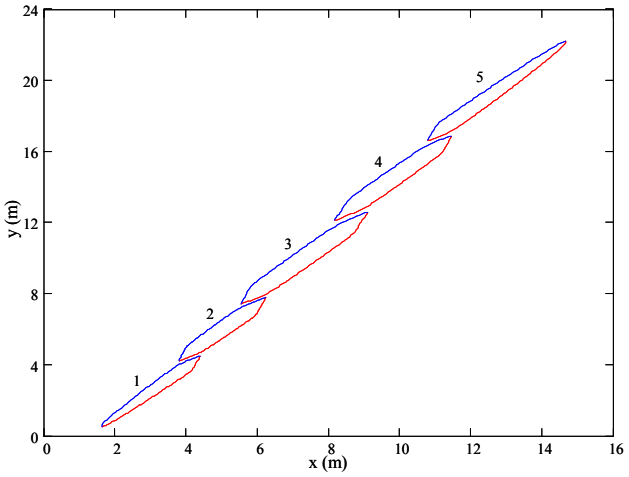

Figure 7. Geometry and opening of five consecutive overlapping segments

For the comparison of the opening with non-interacting single segment, normalized openings of interacting segments are also shown in Figure 8a. This figure shows that all segments are dilated so that the interaction makes all the segments opening wider in this case.

It is expected that the longest segments always have the widest aperture because the aperture is proportional to the segment length, c, in the case of non-interacting single fracture as in (9). However, as shown in the actual segment opening (Figure 8b), the longest segments do not always have the widest aperture because of interaction. The length of segment 3 is smaller than that of segment 5 but

the maximum opening of segment 3 is bigger than that of segment 5 because of the effect of interaction.

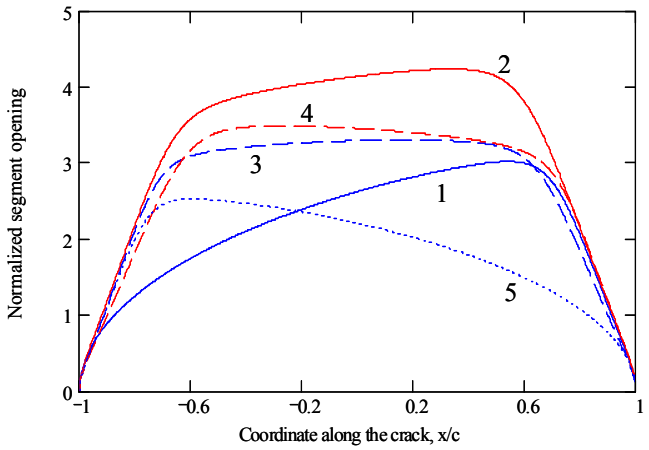

(a) Normalized segment opening

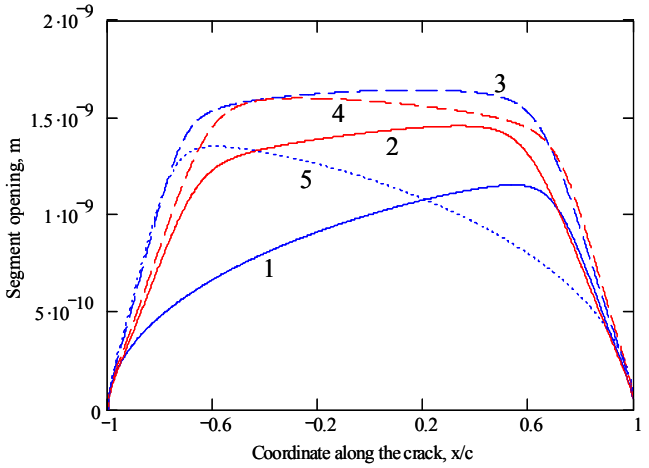

(b) Actual segment opening

Figure 8. Segment opening for five consecutive overlapping segments

4.4 Vertically spaced MHF

In the case of five vertical segments with equal spacing, $S = 0.4$ m and the same half length, $c = 1$ m, and the equal internal pressure, $p = 1.0$ Pa is applied to each fracture and Poisson's ratio $\nu = 0.21$ and Young's modulus $E = 2.5 \times 10^{10}$ Pa are selected (Figure 9). In this structure, the opening of the all the segments are contracted because of interaction (Figure 10a). Therefore, ignoring interaction overestimates the opening deformation in this model.

Besides, edge fractures (segment 1 and segment 5) have the widest opening at the center while neighboring segments (segment 2 and segment 4) are the smallest (Figure 10b). This structure of vertically spaced parallel MHF is also commonly found in nature (see Figure 1d). Accordingly, the permeability of the joint rock mainly depends on the edge fractures in nature.

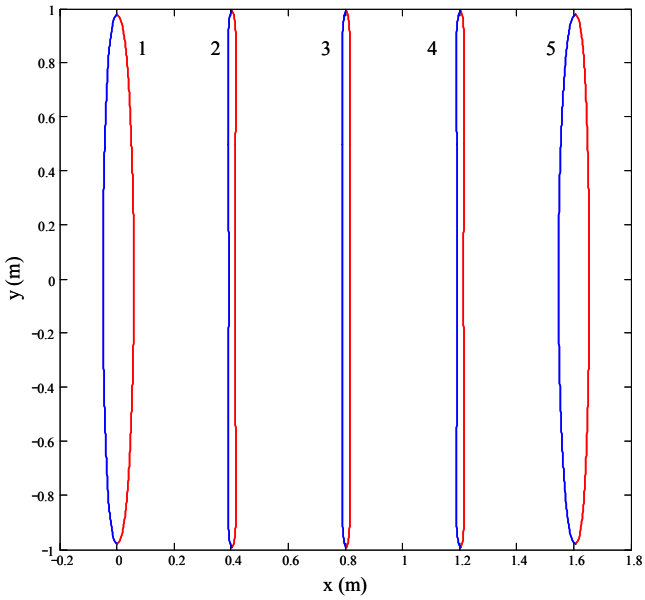

Figure 9. Geometry and opening of five vertical segments.

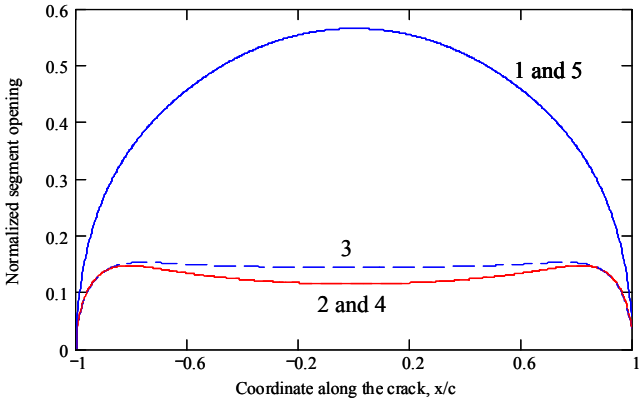

(a) Normalized segment opening

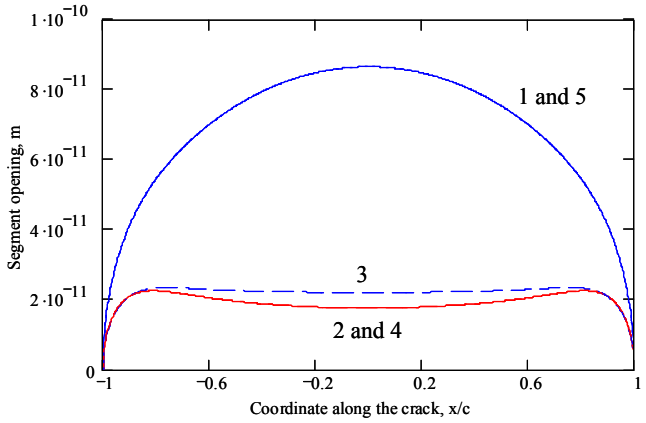

(b) Actual segment opening

Figure 10. Segment opening for five vertical segments

5. CONCLUSIONS

In this study, we obtain following conclusions:

(1) The segmentation by hydraulic fracturing is a common phenomenon in rock. This formation of MHF may be attributed to the generic characteristics of unstable fracture growth, material heterogeneity, or mode III (out of plane shear) mechanisms of fracture segmentation.

(2) The BCM is introduced to evaluate the mechanical interaction between fractures.

(3) Because of the interaction, the same set of fractures in rock shows different opening deformation with a different set of stress condition. The opening of the fracture could be closed.

(4) Because of the interaction, the openings of all segments are bigger than those of non-interacting single segments in consecutive overlapping MHF. The longest fracture does not always have the largest opening deformation, whereas non-interacting single fracture has the largest.

(5) Because of the interaction, the edge fractures in vertically spaced MHF have the largest opening while the inner fractures have the smallest. Ignoring the effect of interaction overestimates the opening deformation in vertically spaced MHF.

(6) Finally, it can be concluded that the mechanical interaction between fractures considerably affects fracture deformation in rock.

(접수일자 : 2006년 1월 4일)

References

1. Anderson, E.M.(1938), The dynamics of sheet intrusion, Proceedings of Royal Society of Edinburgh. Section B, Vol. 58, No. 3, pp. 242~251.
2. Astakhov, D.K.(2000), Permeability Evolution as a Result of Fluid Rock Interaction. Ph.D. Thesis, Georgia Institute of Technology.
3. Beach, A.(1977), Vein arrays, hydraulic fractures and pressure-solution structures in a deformed flysch sequence. S.W. England, Tectonophysics, Vol. 40, pp. 201~225.
4. Delaney, P.T. and Pollard, D.D.(1981), Deformation of host rocks and flow of magma during growth of minette dikes and breccia-bearing intrusions near Ship Rock. New Mexico, Geological Survey Professional Paper 1202.
5. Dudley, J.W., Shlyapobersky, J., Stanbery, R.B., Chudnovsky, A., Gorelik, M., Wen, Z., Glaser, S., Hand, M.K., and Weiss, G.(1995), Laboratory investigation of fracture processes in hydraulic fracturing. GRI, Annual Report.
6. Economides, M.J. and Nolte, K.G.(2000), Reservoir Stimulation. 3rd Edition, John Wiley & Sons.
7. Erdogan, F. and Gupta, G.D.(1972), On the Numerical Solution of Singular Integral Equations. The Quarterly

Journal of Pure and Applied mathematics, Vol. 29, pp. 525～534.
8. Ficher, D.M. and Brantley, S.L.(1992), Models of quartz overgrowth and vein formation: deformation and episodic fluid flow in an ancient subduction zone. Journal of Geophysical research, Vol. 97, No. B13, pp. 20043～20061.
9. Germanovich, L. N., Astakhov, D.K., Shlyapobersky, J., Mayerhofer, M.J., Dupont, C., and Ring, L.M.(1998), Modeling Multisegmented hydraulic fracture in two extreme cases: no leakoff and dominating leakoff, International Journal of Rock Mechanics and Mining Sciences, Vol. 35, No. 4～5.
10. Gladwell, G.M.L. and England, A.H.(1977), Orthogonal polynomial solutions to some mixed boundary-value problems in elasticity theory. Quarterly Journal of Mechanics and Applied Mathematics, Vol. 30, pp. 175～185.
11. Hanson, M.E., Shaffer, R.J., and Anderson, G.D.(1981), Effects of various parameters on hydraulic fracturing geometry. Society of Petroleum Engineers Journal, pp. 435～443.
12. Hubbert, M.K. and Willis, D.G.(1957), Mechanics of hydraulic fracturing, Petroleum Transactions, AIME, Vol. 210, pp. 153～166.
13. Keck, R.G., Fletcher, P.A., and Withers, R.J.(1996), A field demonstration of hydraulic fracturing for solids waste disposal, Part one: injection operations and engineering data analysis, Deep Injection Disposal of Hazardous and Industrial Waste, Scientific and Engineering Aspects. edited by J.A. Apps and C.-F. Tsang, Academic Press, San Diego, pp. 775.
14. McCartney, L.N. and Gorley, T.A.E.(1987), Complex variable method of calculating stress intensity factors for cracks in plates, Numerical Methods in Fracture Mechanics. Proceeding of the 4th International Conference, San Antonio, pp. 55～72.
15. Murdoch, L.C. and Slack, W.W.(2002), Forms of hydraulic fractures in shallow fine-grained formations. Journal of Geotechnical and Geoenvironmental Engineering, Vol. 128, No. 6, pp. 479～487.
16. Muskhelishvili, N.I.(1953), Some basic problems of the mathematical theory of elasticity. Noordhoff, Groningen.
17. Naceur, K.B. and Roegiers, J.-C.(1990), Design of fracturing treatments in multilayered formations. SPE Production Engineering, pp. 21～26.
18. Nemat-Nasser, S.(1983), Thermally induced cracks and heat extraction from hot dry rocks. in Mechanics of Elastic and Inelastic Solids 5, Hydraulic Fracturing and Geothermal Energy, Martinus Nijhoff Publishers, pp. 528
19. Palmer, I.D. and Sparks, D.P.(1991), Measurement of induced fractures by downhole TV camera in black warrior basin coalbeds. Journal of Petroleum Technology, pp. 270～275 and pp. 326～328.
20. Pollard, D.D. and Aydin, A.(1988), Progress in understanding jointing over the past century. Geological Society of America Bulletin, Vol. 100, pp. 1181～1204.
21. Sagy, A., Reches, Z. and Roman, I.(2001), Dynamic fracturing: field and experimental observations. Journal of Structural Geology, Vol. 23, pp. 1223～1239.
22. Secor, D.T.(1965), Role of fluid pressure in jointing, American Journal of Science. Vol. 263, pp. 633～646.
23. Shin, K., Sugawara, K., and Okubo, S.(2001), Application of weibull's theory to estimating in situ maximum stress σH by hydrofracturing. International Journal of Rock Mechanics & Mining Sciences, Vol. 38, pp. 423～420.
24. Tada, H., Paris, P.C., and Irwin, G.R.(1985), The Stress analysis of cracks handbook. Paris Productions Incorporated, St. Louis, Mo.